

Pressure Drop and Heat Transfer in an Isothermal Channel with Impinging Flow

Catharina R. Biber, Ph.D.

Keywords: Heat sink, impinging flow, isothermal channel, pressure drop, heat transfer, electronics cooling

ABSTRACT

The performance of air-cooled plate-fin heat sinks in impinging flow differs significantly from that of similar heat sinks in parallel flow. A numerical experiment and analytical scaling has been carried out to determine the pressure drop and thermal performance of single isothermal channels with variable-width impinging flow. The flow enters the channel normal to the heat sink base. The pressure drop and thermal performance of the flow in this configuration are particularly important for analyzing plate-fin heat sinks for which axial fans supply the flow, since the fan flow rate varies with the static pressure. The results of the numerical experiment and scaling are combined into dimensionless correlations for pressure loss coefficient and channel average Nusselt number. These correlations may then be used to predict the thermal performance of the heat sink.

NOMENCLATURE

D_h	Hydraulic diameter
H	Fin height
K	Pressure loss coefficient (eq. 1)
k	Thermal conductivity of air
L	Flow length
Nu	Nusselt number (eq. 3)
q	Total heat flux over entire channel
Re	Reynolds number, $\rho U D_h / \mu$
s	Channel spacing
ΔT	Temperature rise
U	Average impingement velocity
W	Inlet width
x^+	Flow development length
x_f	Flow development length
x_t	Thermal development length
ρ	Density of air
μ	Dynamic viscosity of air

I. INTRODUCTION

There has been increasing interest of late in enhancing the performance of air cooled plate-fin heat sinks by applying impinging, rather than parallel, flow to the fin channels. Impinging flow implies that the air flow approaches the heat sink perpendicular to the heat sink base. Many such products are appearing on the market for both integrated circuit and power electronics applications. Several recent papers also point to this increased interest [1]-[4]. Most of these papers, however, approach the subject from the total performance point of view. That is, heat sink performance is presented without applying a dimensional scheme by which the engineer could apply a similar analysis to a

heat sink of a different geometry or boundary conditions. For example, Kang et al [1] analytically, computationally and experimentally studied a half-channel with impinging flow in eight different geometries and correlated the resulting thermal resistance and pressure drop for a complete heat sink. They used only one fin spacing, however, and the results are not presented in a form useful for design purposes. Mansuria et al [2] compared straight-fin, pin-fin, and radial-fin heat sinks in impinging flow. Their study used both computational and experimental methods but was restricted to a fixed base area. They did, however, present average heat transfer coefficients in addition to pressure drop and total thermal resistance data. Sathe et al [3] did a computational and experimental study of a heat sink with a notched center slot with impingement cooling. Bailey et al [4] studied the effect of ribs on the performance and pressure drop of channels; their data for smooth channels covers only three Reynolds numbers in a single geometric configuration.

The present study obtains correlations for the average static pressure loss coefficient across the slot jet and for the total heat transfer from an isothermal channel. Figure 1 shows the configuration and defines the geometry. The channel height H , the inlet width W , channel spacing s , channel length L and impingement velocity U vary over significant ranges. Table 1 gives the ranges for each variable.

The intent of the study is to obtain generalized performance indicators that can be used to analyze plate-fin heat sinks for various fin heights, number of fins, and flow lengths when such a heat sink has impinging flow. This type of flow is particularly interesting when supplied by a fan. In that case, the flow length varies for each channel on the heat sink. Although all the channels are the same length, the presence of the fan hub (and the absence of significant net flow under it) reduces the effective flow length in the channel. A set of dimensionless correlations can then be applied to each channel to obtain the pressure drop characteristics of the heat sink. The fan operating point can then be determined. Once the velocity in each channel is known, the correlations can be applied again to predict the total thermal resistance of the heat sink.

II. NUMERICAL EXPERIMENT

A numerical experiment was carried out using a

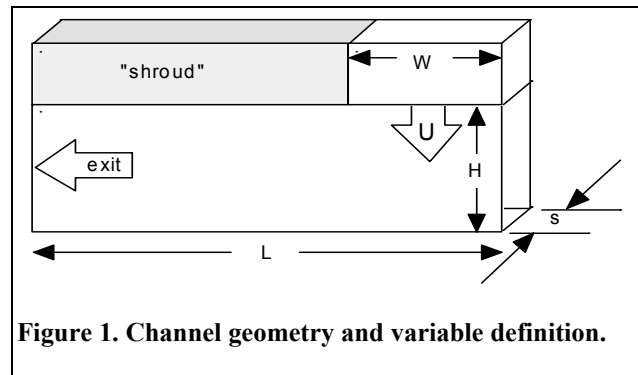


Table 1. Variable Ranges		
Variable	Low	High
H	2.5 cm	5.0 cm
W	1 cm	5 cm
s	1 mm	5 mm
L	5 cm	10 cm
U	1 m/s	5 m/s

commercial finite-volume computational fluid dynamics program. The equations for continuity, momentum in three directions, and energy are solved using the Boussinesq approximation [5].

The analysis covered a single channel with variable spacing s , inlet velocity U , flow length L , and inlet flow width W . Because of symmetry, the domain was half the width of the channel. The channel centerline was an adiabatic, impervious, frictionless plane. To simplify the problem without sacrificing relevance to the practical goal, the boundary representing the channel wall, as well as the floor of the channel, were isothermal. For extruded aluminum heat sinks, as well as most more advanced heat sink types, the fin efficiency is usually high enough to justify this assumption. If the fin is far from isothermal, the approximate calculations for which the correlation will be used can be corrected for fin efficiency in the usual manner [6].

The isothermal wall extended the specified flow length L within a somewhat longer domain. The beginning of the flow length was along a frictionless, adiabatic symmetry plane, to simulate the low-velocity recirculating flow under the fan hub. The impinging flow began 1 cm above the top of the isothermal wall, separated from the wall by an adiabatic, frictionless surface. The exit area was constrained to be the channel height H by an adiabatic solid block with friction. This corresponds to a shroud (see Figure 1) around the fan and heat sink and serves to contain the flow to the heat transfer area.

Sufficient grid was used that the measured parameters were within 1% of the next-finer grid. The grid independence was checked for several, although not all, representative cases. Some accuracy was sacrificed for speed of execution. All of the cases achieved standard convergence criteria.

Most of the cases were laminar flow; for the few with sufficiently high Reynolds number, a k - ϵ turbulence model [4] was applied. Grid independence was especially difficult to achieve in three of these turbulent cases. Again some accuracy was traded off in favor of obtaining results in a reasonable time period.

Forty-three separate cases in a CCF experimental design covered three values for each of the five variables. The results of each case comprised the average static pressure over the inlet width W and the total heat flux transferred by the isothermal walls. The wall temperature was 10 °C above the inlet temperature in all cases.

III. ANALYTICAL APPROACH

For pressure drop, the conventional loss coefficient was used, i.e.

$$K = \frac{\Delta p}{\frac{1}{2} \rho U^2}.$$

In the limit of very short flow lengths, the pressure drop should approach the pressure drop for a simple 90 ° bend, $K = 1$. For very long flow lengths, the pressure drop should vary linearly with the

length as for Poiseuille flow between parallel plates, $\Delta p \sim \rho LU/D_h^2$. Similarly, the velocity dependence of the pressure loss coefficient for laminar flow should approach that for fully developed flow,

$$K \propto \frac{L}{D_h \text{Re}}.$$

Therefore, a length scaling similar to that for developing flow, which satisfies both limits, was chosen to be $x_f = (L^*/D_h)/\text{Re}$. In this case L^* represents an average flow length, D_h is the hydraulic diameter of the channel, $D_h = 4sH/(2s+2H)$, and Re is a Reynolds number based on the inlet velocity.

The heat transfer behavior follows similar analytical arguments. The Nusselt number is defined here as

$$\text{Nu} = \frac{qD_h}{(2H+s)L\Delta T k}$$

where q is the total heat flux transferred from a single channel: both side walls and the channel base, i.e. over an area $(2H+s)L$. Note that this Nusselt number includes the effect of air heating. For heat sink design, the engineer normally has to include an extra calculation for the log-mean temperature difference to account for air heating. Defining the Nusselt number in terms of overall temperatures and heat fluxes saves the engineer a step.

By setting the heat flux equal to the heat absorbed by the fluid, $(\rho U W s)c_p \Delta T_{\text{air}}$, we can obtain a sensible scaling law for the Nusselt number, i.e.

$$\text{Nu} \propto \text{Re} \frac{D_h}{L} \frac{W}{H} \frac{\Delta T_{\text{air}}}{\Delta T_{\text{wall}}}$$

for $D_h = 2s$, $2H \gg s$ and constant Prandtl number.

Thus, for short channel lengths, we should be able to use a developing-flow length definition, $x^+ = (L/D_h)/\text{Re}$, perhaps scaled by W/H . The $\text{Re}(W/H)$ scaling turns out to be the Reynolds number based on the average exit velocity. For very long channels, where the air temperature rise nearly equals the wall temperature rise, we then expect to see $\text{Nu} \sim (x^+)^{-1}$. Equation (4) predicts this scaling. For shorter channels, we expect a smaller negative exponent, similar to developing flow in parallel channels. A curve fit to the data given in [7] shows that Nu scales as $(x^+)^{-0.41}$ in developing laminar flow.

IV. RESULTS

Typical flow patterns obtained in the modeling are shown in Figures 2 through 4. In some cases, as in Figures 2 and 4, a recirculation zone abuts the “shroud” block near the channel entrance. In others, as in Figure 3, the impinging jet accelerates near the same corner. The flow patterns are not distributed in any noticeable way with the traditional scaling parameters.

By proper use of scaling, as introduced above, the data points for the 43 numerical experiments can

be made to collapse onto one curve for the adjusted pressure loss coefficient as a function of the flow development length. Small revisions in the definition of the developing flow lengths improve the curve fit. Replacing L by $(L-W+H)$ gives the best fit. This replacement is justifiable if one imagines a typical streamline, for example near the edge of the impinging slot jet. This streamline length is better approximated by the L-shaped path of height H and length $(L-W)$ after a 90 degree turn. Another modification was made to the correlation to account for the exit velocity instead of the inlet velocity U . From mass conservation, $U_{\text{exit}} = U(W/H)$. Replacing U with U_{exit} in the definition of K leads to the combination $K(H/W)^2$. Similarly, using U_{exit} in the definition of Reynolds number leads to the (H/W) factor in the numerator of x_f .

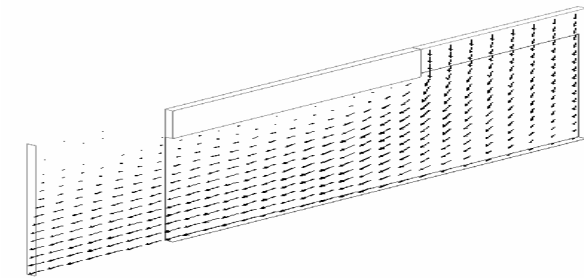


Figure 2. Velocity profile in half-channel.

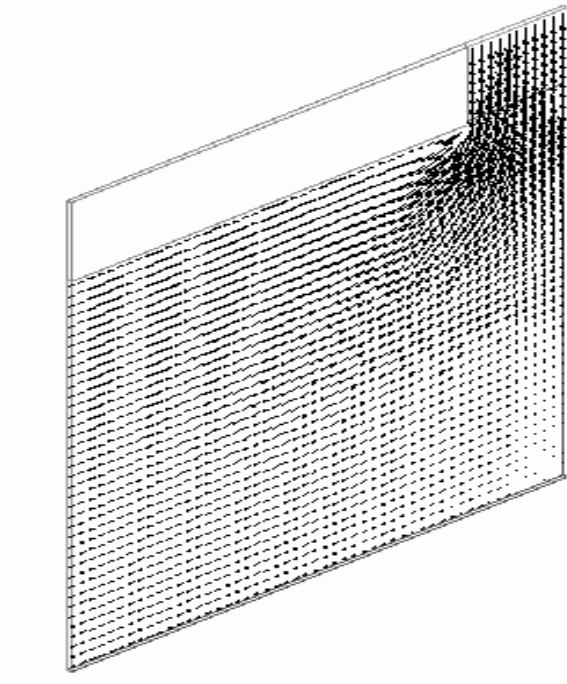


Figure 3. Note flow acceleration at shroud corner.

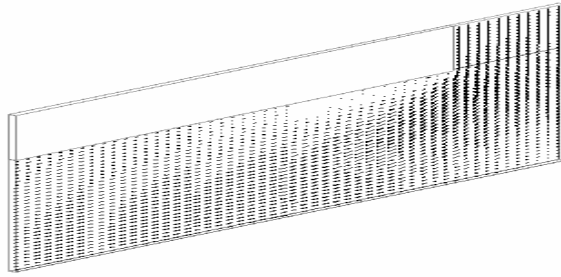


Figure 4. Note flow separation below shroud.

The resulting correlation for the pressure loss coefficient is

$$K\left(\frac{H}{W}\right)^2 = \left[(8.5 x_f^{0.25})^7 + (75 x_f^{1.05})^7 \right]^{1/7}$$

with

$$x_f = \frac{L - W + H}{DRe} \frac{H}{W}$$

The heat transfer scaling also collapses all of the data points:

$$Nu = \left[(6.05 x_t^{-0.22})^{-3/4} + (0.20 x_t^{-1.05})^{-3/4} \right]^{-4/3}$$

with

$$x_t = \frac{L}{DRe} \frac{H}{W}$$

These correlations fit the results of the numerical experiment within $\pm 24\%$ for pressure and $\pm 16\%$ for heat transfer. The data and correlations are shown in Figures 5 and 6.

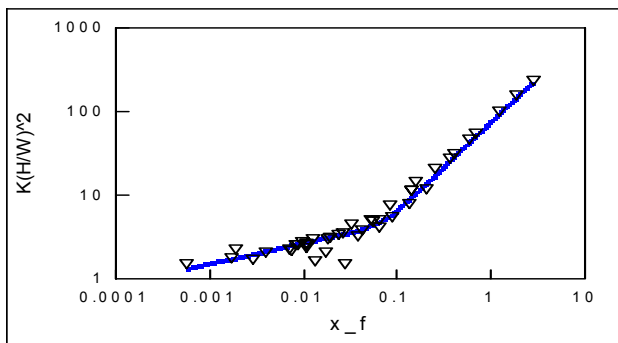


Figure 5. Scaled pressure drop data.

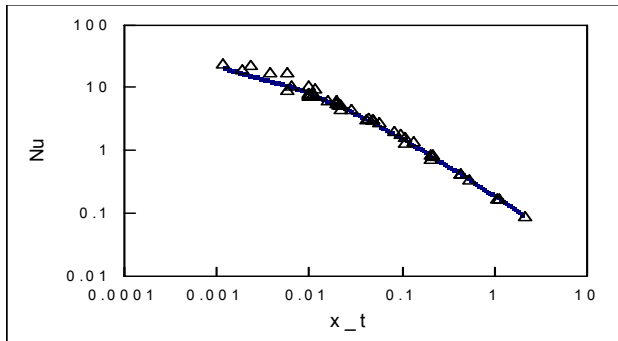


Figure 6. Scaled heat transfer data.

The true measure of the utility of a correlation, however, is not in how well it predicts numerical measurement for ten different test cases. The test cases covered a size range from approximately 3 cm to 21 cm edge length, with fin height ranging from 0.7 cm to 3.6 cm. Some of the heat sinks were rectangular, while others were square. The pressure calculation was used to determine the fan operating point by assuming uniform pressure in the plane above the fin tips. Then the thermal performance was calculated.

In Figure 7, the dark bars indicate the experimentally obtained thermal performance for each heat sink and fan assembly. The light bars show the predictions obtained from the correlations given in this paper. The solid line shows the relative difference between the prediction and the experimental value. The worst agreement, approaching 20% error, were test cases A and B, which had non-uniform channel spacing. The approximate performance prediction assumed uniform channel spacing.

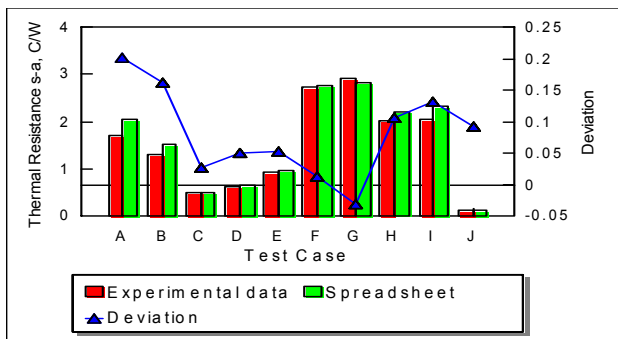


Figure 7. Comparison to experimental measurements.

V. CONCLUSIONS

New correlations for pressure loss coefficient and total heat transfer in a variable-length channel with impinging flow are presented. These numerically obtained correlations cover a wide range of practical plate-fin heat sinks with air supplied by axial fans or other uniform or non-uniform method. When using an axial fan it is especially important to consider pressure drop through the heat sink, since it will determine the fan operating point. Experimental verification of ten different heat sinks

with axial fans shows that the correlations as implemented give good predictions of heat sink thermal resistance.

ACKNOWLEDGMENT

The author wishes to thank Rudi Cartuyvels of IMEC, Leuven, Belgium for a demonstration copy of Norman/Debora software for numerical experiments.

This paper was presented at SemiTherm XIII, Austin, TX, January 30, 1997, and published in the IEEE Transactions on Components, Packaging, and Manufacturing Technology Part A: Components and Packaging Technologies, December 1997, Volume 20, Number 04, p. 458.

REFERENCES

1. S. S. Kang and M. F. Holahan, "Impingement Heat Sinks for Air Cooled High Power Electronic Modules," ASME HTD-Vol. 303, Proceedings of the 30th 1995 National Heat Transfer Conference, Vol. 1, pp. 139-146, Portland, OR, August 1995.
2. M. S. Mansuria and V. Kamath, "Design Optimization of a High-Performance Heat Sink/Fan Assembly," ASME HTD-Vol. 292, Heat Transfer in Electronic Systems (presented at the 1994 International Mechanical Engineering Congress and Exposition), pp. 95-103, Chicago, IL, November 1994.
3. S. Sathe, B. G. Sammakia, A. C. Wong, and H. V. Mahaney, "A Numerical Study of a High Performance Air-Cooled Impingement Heat Sink," ASME HTD-Vol. 303, Proceedings of the 30th 1995 National Heat Transfer Conference, Vol. 1, pp. 43-54, Portland, OR, August 1995.
4. D. A. Bailey and S. E. Lindquist, "Improved Heat Transfer Rates for Impingement Cooling Fins," ASME EEP-Vol. 4-2, Advances in Electronic Packaging 1993, Vol. 2 (Proceedings of the 1993 ASME International Electronics Packaging Conference), pp. 819-826, Binghamton, NY, September 29 - October 2, 1993.
5. Flotherm™ Reference Manual, ©1994 Flomerics Ltd, Surrey, England.
6. F. White, Heat and Mass Transfer, Addison-Wesley, 1991.
7. E. Guyer, Ed., Handbook of Applied Thermal Design, McGraw-Hill, 1989.